ChemPubSoc Europe

DOI: 10.1002/slct.201801423

Chemistry SELECT Reviews

Materials Science inc. Nanomaterials & Polymers

Metal-Organic Framework Nanocrystals

Bráulio Silva Barros,[a] Otávio José de Lima Neto,[b] Allana Christina de Oliveira Frós,[b] and Joanna Kulesza*[b]

Metal-organic frameworks (MOFs) comprise a broad class of crystalline materials defined as porous networks consisting of metal ions or clusters interconnected through polytopic organic linkers. Due to their intriguing structural and topological characteristics which usually offer high surface areas and tunable pore size, MOFs are excellent candidates for a great variety of applications, such as gas adsorption and separation, catalysis, magnetism, photoluminescence and many others. Although attractive, traditional bulk crystalline MOF materials do not always fulfill the specific needs for some applications, such as smart membranes, thin films devices, and drug delivery. Moreover, nanocrystals display properties that differ from the bulk material due to the high surface-to-volume ratio and quantum size effects. Thus, MOF nanocrystals will possibly present new and exciting properties or at least enhance the already known ones. With this view, it is necessary to develop efficient strategies towards the synthesis of MOF nanocrystals. This review provides general concepts of MOF nanocrystals and a critical summary of synthetic approaches with the focus on recent progress in the fabrication of MOF nanocrystals.

Introduction

Nanocrystals

A nanocrystal is a solid particle presenting at least one dimension in the nanometric scale or, most specifically, between 3 and 100 nm (1 nm = 10^{-9} m). At this range of size, solids usually show intriguing and unusual properties, which differ from the properties at the macroscopic level, also known as bulk properties. These outstanding properties are of great interest for the development of many new technologies in fields like medicine,[1] biotechnology,[2] energy[3] and environmental remediation,[4] to give a few examples. Although very important, the size is not the only characteristic of the nanocrystal that affects the properties of solids at the nanoscale. Morphology and state of agglomeration are similarly relevant. The morphology is related to the form of the crystals and how the size varies in the three dimensions of the volume of the solid. Sometimes those nanocrystals, independent of their morphology, may be found in an agglomerated state forming a polycrystal.[5] The term nanoparticle is very often used to designate both polycrystals and single-crystals.

From a historical point of view, the effects of the nanocrystals size on the properties of solids have been observed for a long time. One of the most known examples is the Lycurgus Cup, a 1.600-year-old glass chalice that bears a scene involving King Lycurgus of Thrace.[6] This chalice appears jade green when reflecting sunlight and red when transmits the light of a source placed inside of the cup. Other interesting case was reported first by Michael Faraday in 1857,[7] who observed the changing in color of gold when forming a colloidal suspension of particles. This work marks the beginning of the modern nanotechnology.[8] However, neither the Romans nor Faraday had a real understanding of those intriguing optical properties. Only later, in XX century, based on the well-established fundamentals of modern chemistry and physics as well as the development of advanced characterization techniques such as the electron microscope, it was possible to understand and explain the unusual properties of some materials. Nowadays, we know that the Lycurgus cup was impregnated with silver and gold nanocrystals as small as 50 nm in diameter while the particles in Faraday's colloidal suspension were smaller than 10 nm.[6,8]

Metal-Organic Frameworks (MOFs)

MOFs are a new class of hybrid crystalline materials composed of inorganic and organic units. In these compounds, the inorganic components, ions or metal clusters, are connected through polydentate organic linkers, giving rise to porous frameworks that extend in two- or three-dimensions.[9,10] The vast number of different types of inorganic and organic units leads to almost infinite possibilities of design and synthesis of new hybrid structures. In the last years, the number of new MOF structures deposited in the Cambridge Structural Databases (CSD) has increased exponentially, reaching over 81.000 entries in the update of May 2017.[11] Because of their structural and chemical diversity that allows the control over size, shape, and functionality of the pores, MOFs have achieved the highest porosities of all known materials and pore sizes in the range of

[a] *Prof. B. S. Barros*
Departamento de Engenharia Mecânica
Universidade Federal de Pernambuco
Av. Prof. Moraes Rego, 1235 – Cidade Universitária, 50670-901 Recife, Brasil

[b] *O. J. de Lima Neto, A. C. de Oliveira Frós, Prof. Dr. J. Kulesza*
Departamento de Química Fundamental
Universidade de Pernambuco
Av. Prof. Moraes Rego, 1235 – Cidade Universitária, 50670-901 Recife, Brasil
E-mail: joanna.kulesza@ufpe.br

0.3 to 6 nm.[12] Indeed, it is possible to design frameworks with adjustable pores size and shape as well as specific chemical environments through functionalization of the organic linkers. The fundamental principle of the MOFs design lies in the concept previously used for zeolites (porous inorganic frameworks) and next extended to hybrid structures by Hoskins and Robson,[13,14] the building-block strategy. This strategy considers the assembly of organic and inorganic moieties into an extended array using the mutual interactions between those units, encouraging the formation of extended arrays rather than discrete species.[13–15] The possibility to design frameworks with such freedom is an excellent advantage of MOFs over their inorganic correlates, the zeolites. In the case of zeolites, the restricted number of inorganic building-blocks limits the design of new frameworks.

The unique physicochemical properties exhibit by MOFs have attracted considerable attention over the past decades. The scientific development of these materials involves different disciplines, as well as implies in several potential applications in many fields, including magnetism,[16] gas adsorption and separation,[17] drug delivery,[18] catalysis,[19] sensors[20] and luminescent materials.[21] However, in some cases, the use of MOFs faces some technical limitations. For example, in the field of biomedicine, often small size of particles is a fundamental requirement to ensure the necessary interaction with living cells. Thus, particles smaller than 500 nm usually enter the cells by endocytosis against likely phagocytosis for larger ones, or in other words, without destroying the cell.[22–24] Furthermore, the combination of the unique features of the hybrid porous materials with the benefits of nanoscale structures may promote the improvement of the properties already well known from bulk-MOF materials.[23] Therefore, this review aims to provide a general overview of this new class of porous materials and their intrinsic properties, as well as to present the progress in synthetic pathways to prepare MOF nanocrystals. Also, the fundamental concepts involved in the nucleation/growth of nanocrystals and the control of their size and shape are analyzed.

Properties of MOF nanocrystals

As previously discussed in the Introduction, nanomaterials often present intriguing and, sometimes, unexpected properties, different from bulk materials. Indeed, the properties of the materials depend on the size range over which they are measured.[25] A good example is the changing of gold color from yellow to ruby when the dimensions change from the macroscopic to nanoscopic scale. The peculiar behavior of nanomaterials is also related to the state of agglomeration of the nanocrystals. In this way, nanocrystals and polycrystals may show different properties, and therefore it is essential to establish the differences between both. Although nanocrystals are nanoparticles, not all nanoparticles are regarded as nano-

Bráulio Silva Barros received his B.Sc. in Materials Engineering and M.Sc. in Chemical Engineering from Federal University of Campina Grande, Brazil, D.Sc. in Materials Science and Engineering from Federal University of Rio Grande do Norte, Brazil, and Ph.D. in Chemistry of Catalytic Materials from University of Strasbourg, France. Currently, he is an Associated Professor at Federal University of Pernambuco, Brazil, and the leader of the research group Supramolecular and Multifunctional Materials (SupraMMat). His scientific research is focused on nanostructure materials, including functional ceramics and hybrid materials (MOFs).

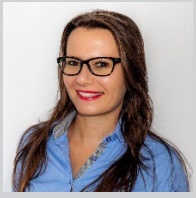

Joanna Kulesza received her M.Sc. in Chemistry (2007) and D.Sc. in Chemistry (2011) from Gdansk University of Technology, Poland, and Ph.D. in Supramolecular Chemistry from University of Strasbourg, France, in 2011. Since 2014, she has been an Adjunct Professor at Federal University of Pernambuco, Brazil and the main member of the research group Supramolecular and Multifunctional Materials (SupraMMat). Her current scientific research is focused on supramolecular nanostructures, including Metal-Organic Frameworks, synthesis, and application in adsorption processes.

Allana Christina de Oliveira Frós received her B.Sc. in Chemistry from Federal University of Amazonas, Brazil in 2010. Currently, she is pursuing her doctorate at Federal University of Pernambuco, Brazil, under the supervision of Prof. Joanna Kulesza. She is a member of the research group Supramolecular and Multifunctional Materials (SupraMMat) where her current research interests focus on the application of Metal-Organic Frameworks for adsorption of volatile organic compounds.

Otávio José de Lima Neto received his B.Sc. in Chemistry from Rural Federal University of Pernambuco, Brazil, in 2015 and M.Sc. in Chemistry from Federal University of Pernambuco, Brazil, in 2018 under the supervision of Prof. Joanna Kulesza and Bráulio Silva Barros. He is a member of the research group Supramolecular and Multifunctional Materials (SupraMMat) since 2016, and his research is focused on the synthesis and application of Metal-Organic Frameworks for drug delivery systems.

crystals. Nanocrystals are characterized by a single-domain crystalline lattice, without the presence of grain boundaries.[26]

Nanoscale-effects

Why make particles as small as possible? We should address this question to get a real understanding of the nanoscale-effects. Although the advantages of nanocrystals have been widely reported over the years, the reasons behind the unique properties of these materials are not always well understood. These properties are size-dependent and can be classified into two types, surface-dominated and size-dominated.[27]

The surface-dominated properties depend on the surface-to-volume ratio. When the size decreases, this ratio increases considerably as well as the total available surface area. Therefore, a most significant number of atoms "matter" is exposed to the environment, affecting both chemical and physical properties.[27] The catalytic properties are a good example; they depend on the interaction of molecules with surface atoms. Thus, nanocrystals with higher surface-to-volume ratio commonly show better catalytic properties. On the other hand, nanocrystals are thermodynamically unstable because the surface atoms are more energetic than those from the volume. As a result, nanocrystals tend to clump to minimize the energy of surface atoms. The agglomeration is not desired once decreases the accessible surface area, mainly in the case of metallic or ionic dense nanocrystals. Porous nanocrystals are probably the best option to overcome this limitation. In the case of MOFs, for instance, the agglomeration of the nanocrystals not necessarily will decrease the available surface area because of their porous lattice.

The size-dominated properties are related to the size of the particles or crystals, and they are particularly fascinating at the nanoscale due to the quantum size effects.[27] The quantum size effects appear when the size decreases to values smaller than 10 nm. In such a tiny crystals electrons and holes are confined forming discrete electronic energy levels rather the energy band structure observed in bulk materials.[28] Additionally, the energy levels separation increases as the nanocrystal size decreases.[28] The change from a band structure to a discrete energy level structure explains, for example, the color of colloidal gold nanocrystals, ruby, which differs from the bulk gold, yellow. The effects of quantum confinement are particularly significant to the optical and electrical properties of the nanocrystals, but also affects other properties.

Applications

MOF nanocrystals are promising candidates in many advanced applications due to the synergistic effect of their intrinsic properties and size. Without any doubt, the most reported applications of MOFs are those related to their adsorption properties such as gas separation and storage, enhanced pollutants adsorption (pesticides and residual drugs).[29,30] However, these materials are much more versatile, and other kinds of applications are found in the literature. Gadolinium-based MOF nanoparticles were tested as MRI (Magnetic Resonance Imaging) contrast agents by Rieter and co-workers.[31] The same authors also studied the performance of manganese-based MOFs as MRI contrast probes.[32] Cadiau and co-workers studied the use of nanoparticles of Lanthanide-based MOFs as luminescent nanothermometers.[33] Recently, Xu and co-workers reported the design of a phosphorescence/fluorescence dual-emissive nanoscale metal−organic framework (NMOF) as an intracellular oxygen sensor.[34] Mori at al. reported the photocatalytic activity of the MOF $[Ru_2(p\text{-}bdc)_2]_n$ (bdc = benzenedicarboxylate) during the hydrogen evolution from water under visible light irradiation.[35]

The interest in the development of MOF nanocrystals is relatively recent, and the opportunities for application in the most diverse fields of science and technology are numerous. As a result, the number of works describing the synthesis, characterization, and the use of nano-MOFs has been growing exponentially in past years. The studies reported here represent just a few of those works focusing on the recent progress in the fabrication of MOF nanocrystals.

Synthesis of MOF nanocrystals

General considerations

MOF nanocrystals may present new or improved properties different from those observed in bulk materials. However, to access these unique features, it is essential to have precise control over the size and shape of matter at the nanoscale. Therefore, a good understanding of the mechanisms involved in the nanocrystals formation is fundamental. Two processes are involved in nanocrystals formation in a liquid medium, nucleation, and growth. The classical theory, LaMer nucleation followed by the Ostwald ripening, is often used to describe the changes in particles size.[36]

LaMer mechanism

According to the classical theory, the nucleation is the first stage of all known crystallization processes and begins with the formation of seeds or nuclei, which play an essential role as templates for the particles growth.[26,36] A seed is a group of few atoms or ions, but in the specific case of MOFs may be better defined as a group of few ions and molecules.

LaMer and co-workers [8] were the first to propose the conceptual separation between nucleation and growth [6]. The LaMer's mechanism tries to explain the crystallization process in three steps.[26,36,37] In the first step, the dissolution of the monomers (ions and organic linkers in the case of MOFs) is considered; consequently, their concentration increases with time. The second step is characterized by the supersaturation of the solution, promoting the interaction between the monomers and allowing the self-nucleation. As a result, the concentration of the monomers in solution drops below the level of supersaturation, and no further nucleation occurs; this is the third step. The seeds grow into nanocrystals until the equilibrium state is reached between the monomers on the surface of the nanocrystal and the monomers in the solution.[26]

Ostwald ripening and digestive ripening

The Ostwald ripening mechanism considers that the particle growth is based on the changes of solubility of the nanocrystals as a function of their size.[38] Smaller nanocrystals with high surface energy redissolve and release their monomers into solution. These monomers, in turn, allow that larger nanocrystals grow still more. On the other hand, in some cases, the opposite effect may be observed when smaller particles grow from the dissolution of larger particles.[36] This mechanism is known as digestive ripening.

Indeed, the nucleation and growth mechanisms of MOF nanocrystals may be much more complicated if we consider other parameters beyond a concentration. Moreover, nowadays, there are different theories for the nucleation and growth of nanocrystals such as the coalescence, the orientated attachment, and the interpenetrated growth.[36] However, these mechanisms are beyond the goals of this section.

MOF synthesis

During the last decade, considerable attention has been paid to design and prepare nanoscale MOFs due to their potential in a variety of applications like imaging, biosensing, biolabeling, and drug delivery. To destine MOF nanocrystals for biomedicine applications, good colloidal stability in an aqueous environment of these nanomaterials is required for efficient intracellular uptake. Typical synthesis procedures, however, result in the formation of bulk MOF powders with commonly large crystal sizes, a wide range of particle size distribution, and irregular shapes.

The preparation of water-stable well-dispersed nano-MOFs remains a synthetic challenge, mostly because the synthesis of MOFs is significantly affected by even subtle variations in reaction conditions. Among the most influencing factors are solvent, temperature, metal precursor, reagents ratio, and concentration. For instance, different metal precursors may not only furnish structurally different frameworks[21] but may also affect the nucleation rate and speed up the formation of MOFs nanocrystals.[39] Temperature effect on the size and distribution of MOF nanoparticles has frequently been studied. For example, Tsai and Langner have reported that as the synthesis temperature was increased from −15 °C to 60 °C, the average particle size on nano-ZIF (ZIF = Zeolitic Imidazolate Framework) decreased (from 78 nm to 26 nm) and narrow particle size distribution was achieved.[40] Nanoscale Eu-btc frameworks (btc = benzenetricarboxylate) with various morphologies, including particle-like, rod-like, straw-sheaf-like nanostructures have been obtained by Dang et al.[41] merely controlling the concentrations of the starting reactants. The choice of an appropriate solvent might be the critical factor in tuning the size of MOF particles. Most commonly used solvents include water, DMF (dimethylformamide), ethanol, and methanol, although more recently acetone has been successfully used in the synthesis of highly porous UiO-66 (UiO = Universitetet i Oslo, University of Oslo) nanocrystals.[42]

This review presents an overview of synthetic techniques and approaches to provide nanoscale MOFs and mostly contains more recent reports from 2017 to 2018. Earlier rapports were partially reviewed in 2015[43] and 2016.[44]

Spontaneous precipitation

Although direct precipitation is one of the simplest methods for the synthesis of MOFs, little has been reported on MOF nanocrystals preparation via this approach.[45] Often, the use of additives is required for the control of size and shape of MOF particles.[46] Our group has prepared nanocrystals of [Cu(1,3-bdc)] MOF (1,3-bdc = 1,3-benzenedicarboxylate) by the rapid precipitation method at room temperature using copper acetate as a precursor source. The synthesis conducted under the same conditions but in the presence of copper nitrate instead of acetate, led to square plate-like microcrystals of the MOF within six months (Figure 1).[47]

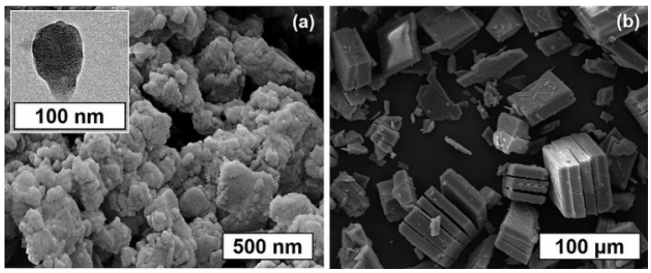

Figure 1. SEM images of Cu(1,3-bdc) MOF prepared using a) copper acetate and b) copper nitrate as a metal source. The inset shows TEM of MOF nanocrystals. Partially adapted from reference.[47] Copyright 2013, Royal Society of Chemistry.

Modification of the direct precipitation called a freeze-drying method is efficient not only in removing solvents without collapse or shrinkage of the structure but also is the promising approach for the preparation of nanocrystals. Wee at al. have first obtained HKUST-1 (HKUST = Hong Kong University of Science and Technology) with narrow particle size distribution in the range of 100 nm – 5 µm from cooled reagents in ethanol-water solvent mixture followed by immediate freezing in liquid nitrogen (–196 °C) and subsequent drying via lyophilization.[48] More recently, Li et al. applied the gel-like cooperated with a freeze-drying method to the synthesis of POM-based MOF (POM = polyoxometalate), MIL-53(Al) (MIL = Materials of Institute Lavoisier) and ZIF-8.[49]

Solvothermal method

In a solvothermal method the reaction precursors are heated up in a sealed autoclave in a high-boiling organic solvent or water; in the latter case, it is called the hydrothermal method. The thermal energy transfer from the heating source to the reaction mixture depends on the thermal conduction of the vessel, and normally the long time of reactions are needed to

achieve the desired temperature. Typically, elevated temperatures and moderate pressures are also required. Such conditions favor the formation of single microcrystals rather than nanocrystals mainly due to the slow nucleation together with fast crystal growth promoted by higher temperatures. Control over precursor ratio and concentration, pressure, time, and temperature can allow the formation of homogeneous nanocrystals. Oveisi et al. have prepared a series of MIL–Ti nano-MOFs by the hydrothermal method.[50] The size and morphology of the particles could be tuned using different molar ratios of bdc/NH_2-bdc linkers (Figure 2). Mixed bdc/NH_2-bdc Ti-MOFs

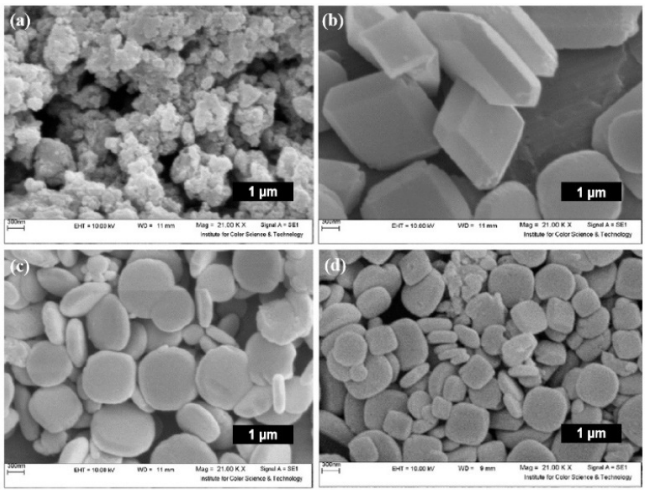

Figure 2. SEM images of the synthesized MILs with different bdc/NH_2-bdc ratio. (a) MIL-125(Ti) (0/100), (b) MIL–X1 (75/25), (c) MIL–X2 (50/50), and (d) NH_2-MIL-125(Ti) (100/0). Adapted with permission from reference.[50] Copyright 2017, Elsevier.

presented morphology change from tetragon (Figure 2b) to circular (Figure 2c) plates with the decreased concentration of the bdc linker.

One of the serious disadvantages of the solvothermal method (and any high-temperature MOFs synthesis in general) is the facilitated oxides formation what impairs the quality of the final MOF product.[51] Careful control of synthesis parameters, especially the temperature of reaction, may avoid the formation of oxide impurities, yet it is a challenging task. Generally, the approaches based on a non-conventional heating source such as microwave or ultrasound, do not face the problem of oxide or salts impurities.

Microwave-assisted synthesis

The particle morphology can be greatly influenced by the concentration and temperature gradient within the reaction medium. These parameters are practically impossible to control during the conventional solvothermal heating. On the other hand, the use of non-conventional heating provided by microwave irradiation is one of the well-known techniques to produce uniform nanocrystals. In this case, two mechanisms, dipole rotation, and ionic conduction are responsible for energy transfer, and so the heating process does not occur through a vessel as in a conventional method.[52] Therefore, the rapid temperature increase causes local superheating providing a huge number of hot spots which can serve as nucleation seeds for crystal growth. Such conditions lead to the formation of small uniform particles. A significant number of papers on nano-MOFs preparation by the microwave-assisted method has been published[53,54] since the first communication in 2005.[55] For instance, Wang et al. have prepared nano-sized (< 100 nm) NH_2-functionalized Zr-MOF (UiO-66-NH_2) *via* a rapid microwave-promoted synthesis and first used in the adsorptive removal of Pb(II) and Cd(II).[56] More recently, Huang el at. have observed that the temperature of microwave-assisted method influenced the morphology and stability of UiO-66-NH_2.[54] With the increase of the synthesis temperature up to 150 °C, the formation of more regular and larger polyhedral nanocrystals could be observed (Figure 3). Further increase of temperature

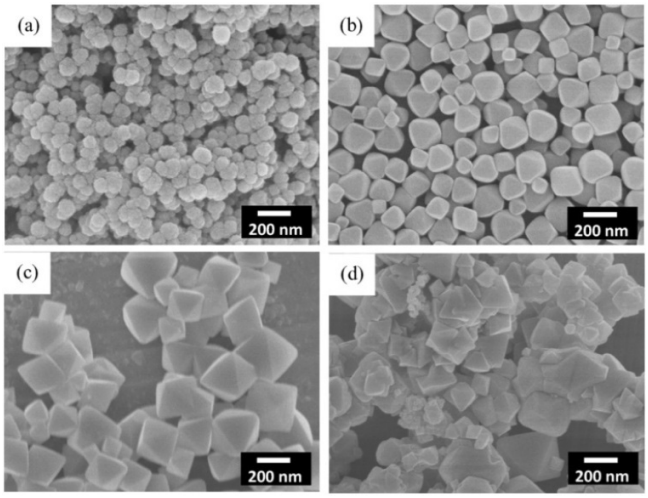

Figure 3. SEM images of the UiO-66-NH_2 prepared by microwave heating for 30 min at a different temperature: (a) 100 °C, (b) 125 °C, (c) 150 °C, (d) 175 °C. Adapted with permission from reference.[54] Copyright 2018, Elsevier.

to 175 °C, led to a slight particles aggregation attributed to a high crystal growth rate.[54]

Benzimidazole-functionalized Zr-UiO-66 (UiO-66-BI) octahedral nanocrystals with a diameter smaller than 200 nm have been successfully fabricated *via* microwave synthesis by Dong et al..[57] The authors demonstrated that UiO-66-BI showed excellent selective luminescent sensing of Fe^{3+} ions in water.

Microwave irradiation of DMF solution containing 0.25 mL of formic acid and $Ni(NO_3)_2.6H_2O$ (0.284 g) led to the formation of nickel-based metal-organic framework $[Ni_3(HCOO)_6]$. The optimized synthesis conditions, DMF content (20 mL) and microwave power (300 W), furnished nano-MOF with high crystallinity and uniform particle size (around 140 nm). The material showed remarkable high specific capacitance (1196.2 F/g) demonstrating its potential application in supercapacitors.[58] Because microwave irradiation interacts only with molecules being polar or ionic, the efficiency of this method

depends greatly on the polarity of solvents and reagents and may present some limitations in non-polar solvents.[52] Moreover, the non-thermal effects of the microwave irradiation on reactions, especially on tuning the morphology of nanomaterials, is still undiscovered and controversial. The non-thermal effects include i.e. the direct interaction of microwave radiation with specific components of the reaction medium. Since both thermal and non-thermal effects exist simultaneously under the microwave irradiation, the influence of the latter one should not be neglected. Therefore, the analysis of microwave irradiation on tuning the morphology of MOF nanocrystals is a much more complex task. This challenging issue has been recently addressed by Laybourn et al. who managed to synthesize well-known MOF material MIL-53 within few seconds (4.3 sec.) *via* microwave irradiation.[59] The authors examined the effect of an average absorbed power with a constant total absorbed energy and defined a selective heating mechanism that allows the control over MOF particle size range and morphology by altering the microwave power.

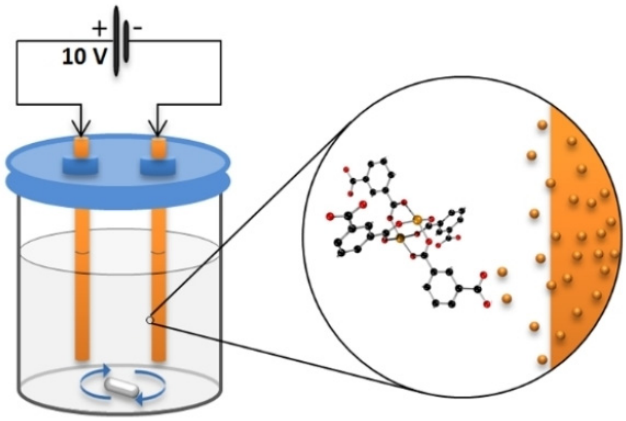

Figure 4. Scheme of the electrosynthesis setup for the preparation of [Cu-1,3-bdc] *via* anodic dissolution. Reproduced with permission from reference.[47] Copyright 2013, Royal Society of Chemistry.

Electrochemical method

There are two main electrochemical methods for obtaining MOFs described as cathodic and anodic. In anodic dissolution, the organic linker is present in the electrolyte solution, and the metal cations are supplied by the oxidation of electrode material. In the cathodic method, metal cations and an organic ligand are both present in the electrolyte solution. During the process, the increased pH causes deprotonation of the organic ligand and subsequent MOF formation. Electrochemical methods have several advantages over conventional MOFs synthesis approaches such as shorter reaction times (typically from a few minutes to 2 hours), milder conditions (usually performed at ambient conditions), no need of using metal salts (in the case of the anodic method), or specialised equipment, and allow controlling the reaction in real-time.

Although very attractive, mostly for the formation of thin MOF films on the electrode surface,[60] studies concerning the cathodic approach in the electrosynthesis of MOFs are less frequent. On the other hand, the anodic dissolution (Figure 4) pioneered by BASF in 2005 is the most common electrochemical method for MOFs preparation.[47,61]

Electrosynthesis parameters such as potential, current density, distance between the electrodes, synthesis time, solvent and electrolyte concentration, all significantly affect the size and shape of MOF particles. Higher values of applied potential promote rapid dissolution and increase metal ion concentration what affords fast nucleation and consequently smaller crystals. Since metal ions are highly hydrated in water, the nucleation rate may be lowered by the presence of increased amount of water in the reaction medium. Consequently, larger crystals might be formed. Therefore, varying the electrosynthesis conditions, the crystal size may be tuned.[62] Commonly, particles obtained by the electrochemical method are smaller than those produced under solvothermal or slow diffusion methods.[47] As a consequence, electrosynthesized MOFs often possess much larger surface area than those obtained by conventional methods. MOFs prepared *via* electrochemical method up to 2014 was reviewed in.[62] Since then, a significant number of electrochemically synthesized MOFs has been announced.[63–66] More recently Zhang et al. have reported the preparation of interesting proton-conductive HKUST-1 films *via* an electrochemical method.[66] The proton conductivity was provoked by the presence of phosphotungstic acid (PTA) molecules inside the MOF cavities. The authors found that MOF films with different thickness and crystal sizes could be prepared by applying different voltages and reaction times (Figure 5).

Contrarily to what should be expected, the crystal sizes increased from 400 nm at 1.0 V to 2.5 μm at 2.0 V as well as the film thickness due to the combination of both, fast nucleation and rapid crystallization considering a high concentration of Cu^{2+} ions between electrodes as the potential increases.

Although the use of electrosynthesis methods for the formation of MOFs is growing rapidly, some critical issues should be concerned. For instance, little is known about the mechanism of the electrosynthesis process, and frequent formation of significant amounts of by-products has been observed. For instance, to avoid the reduction of metal cations, some additives may be used and reduced instead of the ions what prevents the formation of impurities. Also, the use of protic solvents ensures the evolution of hydrogen instead of metal ions reduction what eliminates impurities formation. Although anodic dissolution dispenses the use of metal salts, preventing their adsorption on the surface or incorporation in the MOF pores, conducting salts should be carefully removed from the obtained powders to prevent their entrapment.

Ultrasound-assisted synthesis

Ultrasound (US) is a cyclic mechanical vibration of a frequency between 20 kHz and 10 MHz. When such high-energy radiation interacts with liquids, a phenomenon of acoustic cavitation is observed. This process is based on the formation, growth, and

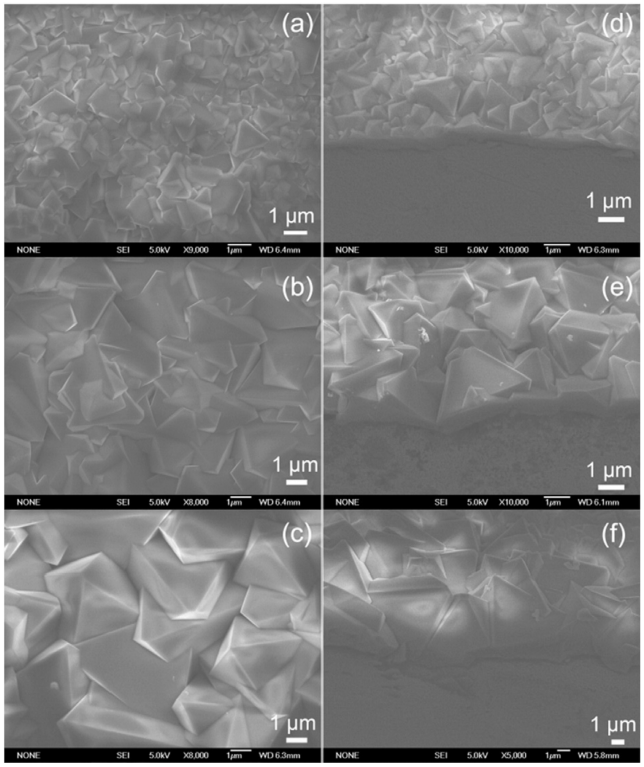

Figure 5. Typical SEM images of the HKUST-1/PTA films prepared on the copper substrates for (a) 0.5 h, (b) 1 h, and (c) 8 h at a given voltage of 2.0 V, respectively; the corresponding SEM images (d-f) of the cross-section views. Reproduced with permission from reference.[66] Copyright 2017, Elsevier.

collapse of bubbles (called cavities). The bubbles grow under alternating pressure through diffusion of solute vapor to bubble volume (when the product is formed), and once they reach their maximum size, they become unstable and collapse immediately (bubble lifetime is around a few microseconds) forming hot spots with temperatures up to 5000 K and 500 atm pressures. Such conditions favor the formation of small and uniform crystallites mostly due to the rapid formation of crystallization nuclei.

Ultrasound-assisted synthesis of MOFs has been performed since 2008 when $Zn_3(btc)_2.12H_2O$ was first obtained.[67] Interestingly, the reaction of zinc acetate with H_3btc under the same conditions but without ultrasonic irradiation failed in producing MOF structure. Not only the ultrasound must play an important role during the formation of MOFs, but the particle shape could also be controlled. The authors showed dimensionality of MOF nanocrystals could be tuned under different reaction time (5 to 90 min) furnishing particles with a diameter ranging from 50 to 900 nm, respectively.

These first results reveal that ultrasonic synthesis is a simple, mild, efficient (high yield, short reaction time), cost-effective, reproducible and environmentally friendly approach (mild conditions) to nanoscale MOFs. Application of ultrasound for the synthesis of nanoscale MOFs was the topic of an extensive review in 2015.[68] Since then, the number of ultrasound-assisted syntheses of MOFs has been increased. It has been reported that the shape and size of Zn(II)-based MOF $[Zn(oba)(4\text{-bpdh})_{0.5}]_n{\cdot}(DMF)_{1.5}$ (oba = 4,4′-oxy bis(benzoate), 4-bpdh = 2,5-bis(4-pyridyl)-3,4-diaza-2,4-hexadiene) could be efficiently tuned by the initial reagents concentration and ultrasonic irradiation time.[69] Unlike in the previous example, in this case, longer exposition on ultrasonic irradiation (90 min) did not provoke the change in morphology, but the separation of microspheres constructed from uniform nanorods was observed (Figure 6).

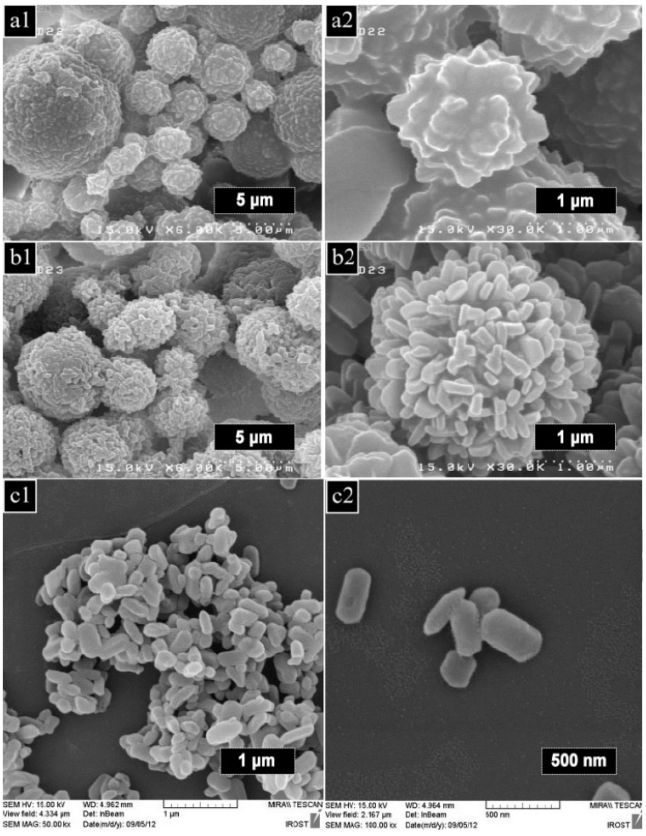

Figure 6. SEM images of nanorods of $[Zn(oba)(4\text{-bpdh})_{0.5}]_n{\cdot}(DMF)_{1.5}$ synthesized by sonochemical reaction for (a) 30 min, (b) 60 min, (c) 90 min. Reproduced with permission from reference.[69] Copyright 2016, Elsevier.

However, the increase of initial reagent concentration led to the formation of larger non-uniform nanorods, whereas the opposite was true for lower initial reagents concentration. Similar conclusions were recently drawn based on a sonochemical synthesis of $[Zn_4(oba)_3(DMF)_2]$.[70] Kim et al., have revealed the formation of the non-interpenetrated PCN-6 framework (PCN = Porous Coordination Network) at lower power levels (150 W) and corresponding interpenetrated PCN-6′ at higher power levels (300 W). At intermediate level (200 W), the mixture of both phases was obtained.[71] The US power level also affected the size of MOF particles; somehow, the interpenetration produced larger crystals. It is well known that interpenetration drastically reduces the surface area of MOFs impairing adsorption features; therefore, the control of this

phenomenon is of significant importance. To our best knowledge, such characteristic has never been observed or investigated using another synthesis method.

Ultrasound-assisted synthesis can be easily combined with other methods and approaches to provide MOFs with desirable properties. Among these combinations, sonoelectrochemical method merges benefits furnished by both approaches such as short reaction time, small and uniform particles, no need of using metal salts, etc. Although technically more sophisticated than US method, sonoelectrochemical synthesis is more environmental-friendly approach and meets the requirements of green chemistry. The first example of the sonoelectrochemical synthesis of MOF was reported by G. G. da Silva et al. in 2016.[72] The nanocrystals of HKUST-1 synthesized by sonoelectrochemical approach were much smaller (crystallites average size of 22–47 nm) than octahedral microcrystals obtained by a conventional solvothermal method with a size around 2–15 μm.

Synthesis of MOFs in the presence of ionic liquids

Ionic liquids (ILs) have attracted considerable attention in the synthesis of MOFs for more than one decade and have been used as solvents, framework structure component,[73] modulators or adsorption-enhancement agents.[74] The increased interest in the use of ionic liquids is mainly attributed to the unique and interesting properties of these compounds. Ionic liquids are salts composed of organic cations and anions counterparts. These solvents are liquids at room temperature, have low volatility, high ionic conductivity and polarity. Nevertheless, their high viscosity and cost are still considered as major obstacles for their use in MOFs synthesis. Liu et al. have obtained ellipsoid-like crystals of NH_2-MIL-53 MOF with a particle size of around 30 nm using 1-ethyl-3-methyl-imidazolium ionic liquid.[75] Sang et al. have revealed the accelerated formation of Zr-based metal-organic frameworks UIO-66 at room temperature in the presence of ionic liquid 1-hexyl-3-methylimidazolium chloride ([Omim]Cl). The reaction time was shortened from at least 120 h (normally required in the synthesis using conventional DMF solvent) to 30 minutes at which time, the samples exhibited good crystallinity.[76] Moreover, this approach led to the formation of nanoscale materials with the particle size of about 80 nm after 60 min crystallization.

MOFs synthesis in the presence of additives

Presence of surfactants

One of the methods to promote small and uniform particles consists of the addition of surfactants or block copolymers. Surfactants are amphiphilic organic compounds containing both water-soluble and water-insoluble components. There are two mechanisms of surfactants action; they can act as capping agents or inhibitors of growth or at certain conditions, they may self-assemble forming micelle-like microreactors. Also, some reports have revealed that surfactants may act as supramolecular templates[77] to obtain metal-organic frameworks with hierarchical porosity. In most cases, by tuning the synthesis conditions, i.e., a surfactant to ligand ratio, smaller nanocrystals further aggregate to mesoporous MOFs. In the other case, the presence of surfactant provoked the conversion of precipitate into a crystalline material.

In each case, care should be taken to posteriorly remove surfactants from MOFs surface. Otherwise, their presence may be a significant interferent, especially for some applications like sensing or drug delivery. The removal of surfactants may become a very laborious procedure including multiple washings and can require severe conditions.

Surfactants as capping agents

Surfactants which act as capping agents adhere to the surface of MOF material hindering the reagents attachment to the surface thus slowing the rate of crystal growth. Park et al. used a triblock copolymer composed of two poly(ethylene glycols) at both of the termini of the poly(propylene oxide) known as Pluronic F127 as a surfactant to enhance the colloidal stability of Tb-MOF nanocrystals in water. The authors found that simple grinding of Tb-MOF with the surfactant in water, followed by sonication furnished Tb-MOF nanocrystals with the average size of 120 nm.[78]

Another widely used surfactant, cetyltrimethylammonium bromide (CTAB), together with a second capping agent, tris (hydroxymethyl)aminomethane (TRIS), were used to obtain ZIF-8 nanocrystals with morphology control in aqueous media.[79] The idea behind this approach is that both surfactants adsorb onto different surface facets of ZIF-8 promoting a variety of morphologies from cubic to octahedral, hexapods, burr puzzles and flower-like shapes by varying the quantity of both agents.

Gao et al. prepared nanosheets of Zn/ibuprofen-based MOF by a solvothermal method using sodium dodecylbenzene sulfonate as a surfactant. Compared to bulk MOF, the obtained MOF nanosheets, with the thickness of about 150 nm (Figure 7), show remarkable pH-controlled ibuprofen release.[80]

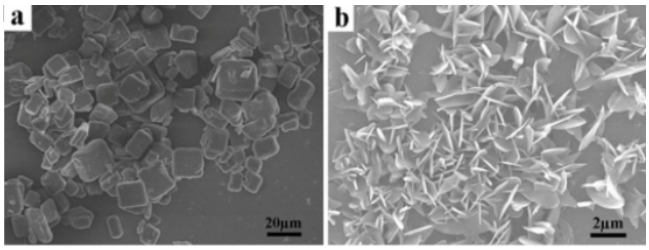

Figure 7. SEM images of Zn-based MOF (a) bulk material, (b) MOF nanosheets. Adapted with permission from reference.[80] Copyright 2017, Elsevier.

Surfactants-assisted synthesis in microemulsions

Surfactant-assisted synthesis in microemulsions is a promising method to control the size and shape of MOF nanocrystals. Increasing number of publications has appeared since the first use of microemulsion approach for the synthesis of $Cu_2[Fe(CN)_6]$ nanoparticles has been reported.[81] Zheng et al. have prepared nanoscale zeolitic imidazolate frameworks (NZIFs) in the ionic liquid microemulsion (ILME) system of H_2O/$BmimPF_6$/TX-100 ($BmimPF_6$ = 1-butyl-3-methylimidazolium hexafluorophosphate, TX-100 = Triton X-100) by a direct mixing method at room temperature as shown in Figure 8.[82]

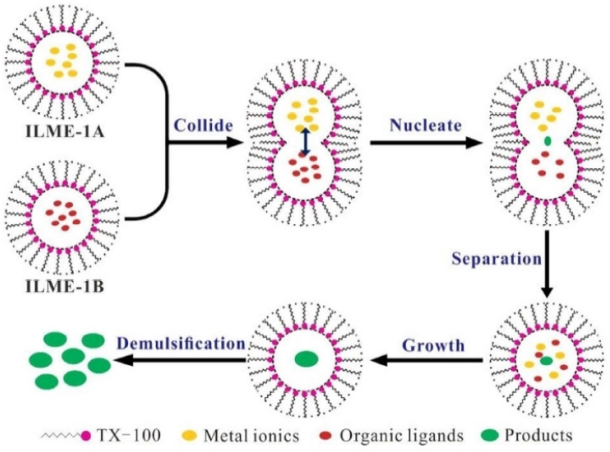

Figure 8. The growth mechanism of ZIFs nanoparticle synthesized in H_2O/$BmimPF_6$/TX-100 (ILME-1). Reproduced with permission from reference.[82] Copyright 2017, American Chemical Society.

The prepared ZIFs nanocrystals had an extremely small size of ca. 2.3 nm and narrow particle distribution of less than 0.5 nm (Figure 9). This approach was also useful in the preparation of nanocrystals of $[Cu_3(btc)_2(H_2O)_3]_n$ (HKUST-1) containing poor water-soluble ligand by the addition of ethanol to the system (ILME-2).

Recently, Sargazi et al. have reported the use of reverse micelle (RM) and ultrasound-assisted reverse micelle (UARM) approaches to synthesize Th-nano MOFs.[83] In a typical reverse micelle method, a surfactant (in this case sodium dodecyl sulfate) is dissolved in an organic solvent (n-hexane) promoting the formation of reversed micelles. The subsequent addition of an aqueous solution of precursors (metal salt and organic ligand) promotes the MOF growth inside of reverse micelles nanoreactors. The authors revealed that the Th-MOF sample synthesized by UARM method had higher thermal stability, smaller mean particle size (27 nm), and larger surface area than samples prepared by RM method. Smaller particle size may be attributed to the fast nucleation rate promoted by ultrasound irradiation. Moreover, the size and shape of Th-MOF samples could be tuned by varying synthesis conditions such as surfactant content, ultrasound duration, temperature and power of ultrasound-assisted reverse micelle method (Figure 10).[83] The synthesis parameters of the UARM method were designed by 2^4 factorial design. For each factor (A – surfactant content [mmol], B – US duration [min], C – temperature [°C], D – US power [W] three levels (superior +1, central point 0, and inferior −1) were established: A - 0.136 (+1), 0.077 (0), 0.018 (-1); B – 30 (+1), 21 (0), 12 (-1); C – 55 (+1), 40 (0), 25 (-1); D – 240 (+1), 175 (0), 110 (-1).

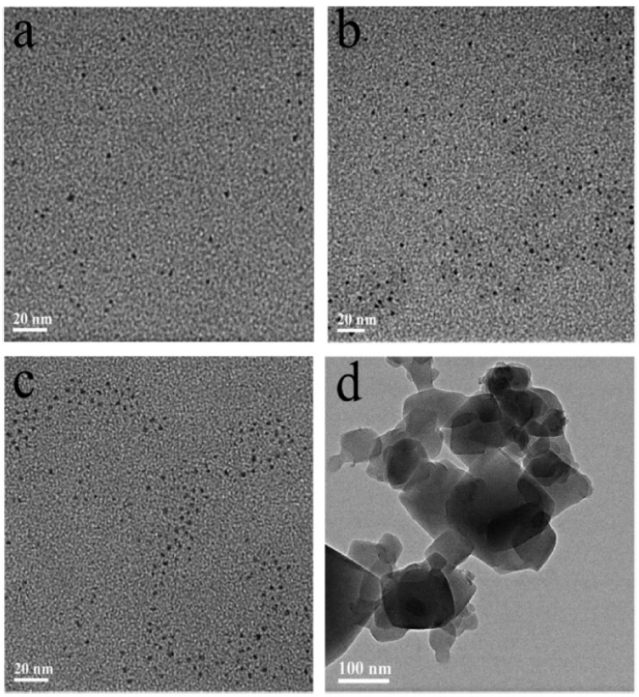

Figure 9. TEM images of (a) NZIF-8 synthesized in ILME-1, (b) NZIF-67 synthesized in ILME-1, (c) NHKUST-1b synthesized in ILME-2, and (d) NHKUST-1a synthesized in ILME-1. Reproduced with permission from reference.[82] Copyright 2017, American Chemical Society.

Analysis of variance (ANOVA) showed that several factors, including surfactant content, ultrasound duration, temperature, ultrasound power, and interaction between these factors, considerably affected different properties of the Th-MOF samples. For instance, the optimal conditions for obtaining minimum particle size and uniform morphology were provided when all these factors were on the central point level (surfactant content 0.077 mmol, US duration 21 minutes, temperature 40 °C, US power 175 W, Figure 10e). When the time of reaction, irradiation time and US power were at the superior level (US duration 30 minutes, temperature 55 °C, US power 240 W, and the surfactant content at low level (0.077 mmol) the particles were strictly agglomerated, and their sizes were in the bulk form (Figure 10b).

Modulators

Non-coordination modulation

Among non-coordinating modulators, basic modulators are the most frequently reported, and their role in the formation of

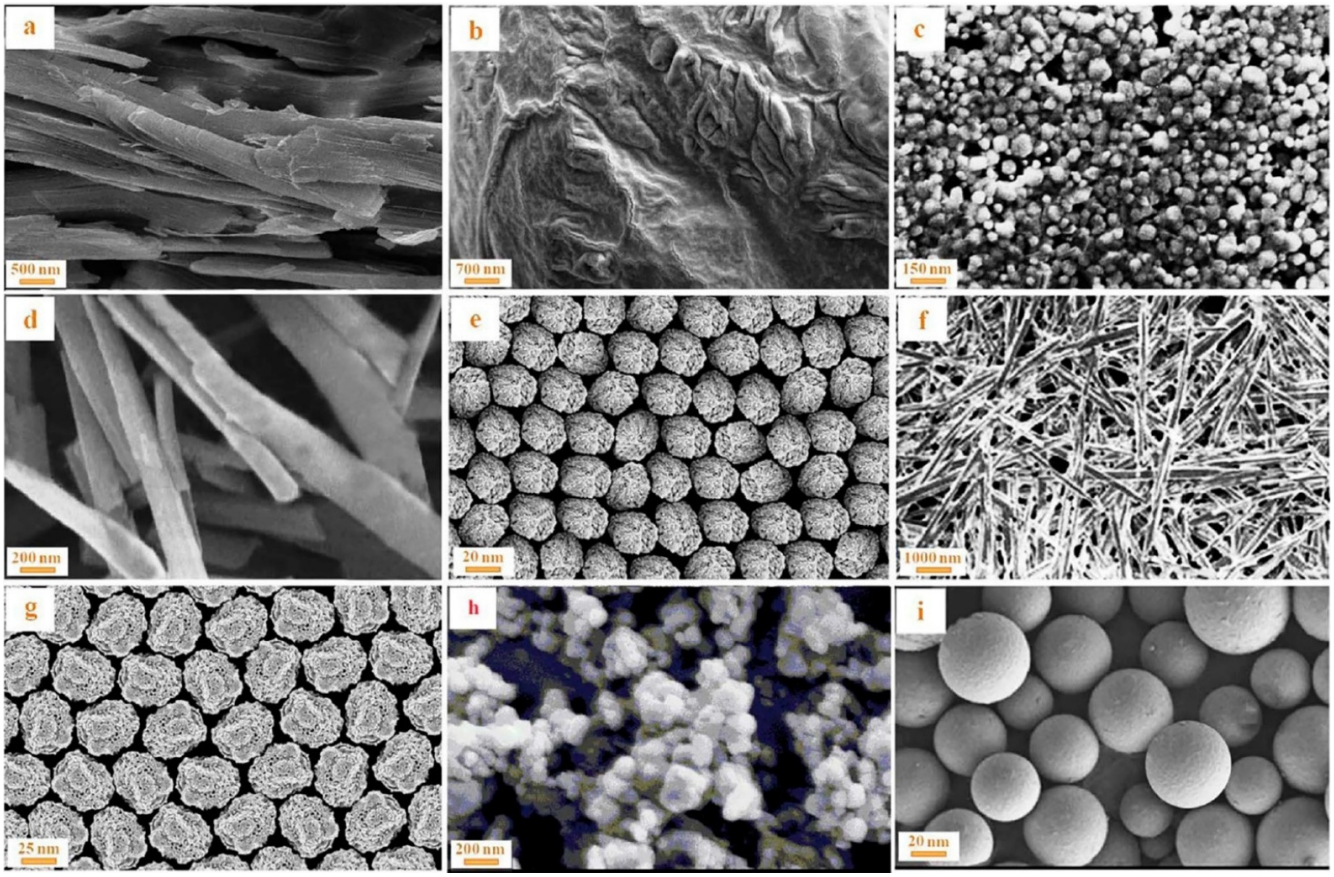

Figure 10. SEM micrographs of Th-MOF samples synthesized under different conditions of ultrasound-assisted reverse micelle method. a) A (+1), B (-1), C (0), D (-1); b) A (-1), B (+1), C (+1), D (+1); c) A (0), B (-1), C (-1), D (+1); d) A (+1), B (0), C (0), D (+1); e) A (0), B (0), C (0), D (0); f) A (-1), B (+1), C (+1), D (0); g) A (0), B (-1), C (0), D (0); h) A (-1), B (0), C (0), D (0); i) A (0), B (-1), C (-1), D (0). Reproduced with permission from reference.[83] Copyright 2017, Elsevier.

small MOFs particles is mostly associated with the acceleration of the nucleation rate. Basic modulators increase pH of the reaction medium, what causes faster deprotonation of the organic linker, and consequently faster MOF formation.

The use of other modulators like HF (currently prohibited in Europe due to the safety reasons) and HCl has also been reported. For instance, Vakili et al. have observed that the presence of HCl in the microwave-assisted synthesis of Zr-based framework UIO-67 led to the accelerated formation of MOF intergrown small crystals. The authors explained that the increased HCl solution used in the UiO-67 synthesis, provided more water in the reaction medium, enhancing the hydrolysis of zirconium precursor and the formation of more Zr-SBUs (SBU = Secondary Building Units) and, consequently the formation of UiO-67.[53] Similar conclusions have been drawn earlier by Katz et al.[84] who have observed the decreased amount of HCl slowed down the UiO-67 MOF formation and decreased the surface area.

Polyethylene glycol 20000 (PEG 20000) and/or MeOH were used as a surfactant to control the size and morphology of nanocrystals of γ-cyclodextrin metal – organic frameworks (γ-CD-MOFs) obtained by the microwave-assisted method by Liu et al..[56]

Coordination modulation

Coordination modulation is one of the most practiced methods for morphology control of MOF nanocrystals. This approach relies on the addition of modulators containing only one functional group able to coordinate to the metal center. According to the proposed coordination modulation mechanism, during the synthesis, modulators (monodentate ligands) compete with polytopic ligand by coordination to metal ions and then, the ligand exchange yields the desired framework. A monodentate ligand that competes with the polydentate linker can limit to a certain extent the growth of the crystal. Thus, the modulator can sometimes act as a capping agent. Commonly used coordination modulators include acetic acid,[10] benzoic acid[85] or dodecanoic acid.[86] Nevertheless, it should be highlighted that the coordination modulation method is not limited to modulating agents with identical functionalities to the organic linker. For instance, Cravillon et al. have employed an excess of the bridging bidentate ligand and various auxiliary monodentate ligands with different chemical functionalities (carboxylate, *N*-heterocycle, alkylamine) in tuning the size and shape of ZIF-8 crystals.[87]

Nanocrystals of $[Zn_2(1,4\text{-bdc})_2(dabco)]$ (dabco = 1,4- diazabicyclo[2.2.2]octane) named as DMOF-1–Zn were successfully prepared by the electrochemical method.[88] The authors found that the size and morphology of DMOF-1-Zn is strongly current dependent. Lower current densities promoted the formation of nanorods, which changed to nanoplates upon the current density up to 0.8 mA cm^{-2}. Further increase of current density up to 1.6 or 4.8 mA cm^{-2} furnished micro-particles. Moreover, the combination of the electrochemical method with the coordination-modulation approach using acetic acid led to the morphology change from microplates to uniform nanorods.

Leite et al. have shown that a gradual increase in acetic acid concentration led to the morphology change from micro-rods to flower-like small particle agglomerates of Mixed Lanthanide-Organic Frameworks (MLOFs). Interestingly, the addition of acetic acid also eliminated the formation of a secondary phase caused by the use of higher total reactants concentrations (Figure 11).[10] Phase-selective surfactant-assisted synthesis of MOFs has also been reported in.[89]

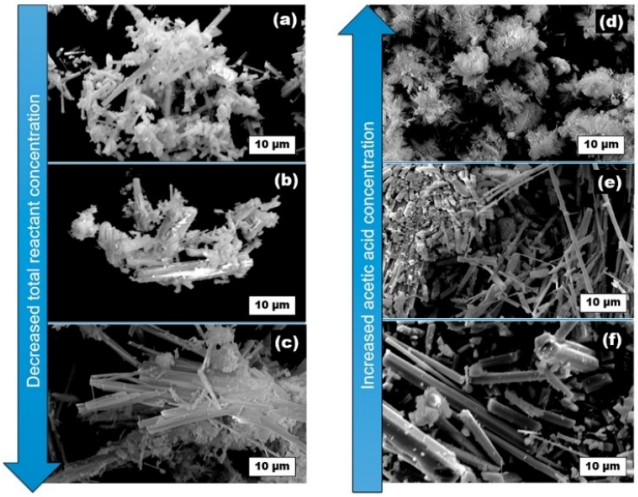

Figure 11. SEM images of $[Ln(HCOO)_3]_n$ MOF samples prepared using the following amounts (in mmol) of Tb^{3+}:La^{3+}:1,3-H_2bdc, (a) 0.02:0.9:1, (b) 0.01:0.49:0.5, (c) 0.002:0.098:0.1 and different acetic acid / distilled water ratios (in mL); (d) 2.0:1.0, (e) 1.5:1.5 and (f) 0.5:2.5.[10]

It should be born in mind, however, that the use of modulators may provoke the formation of structural defects created mainly by the partial ligand-exchange between the polydentate linker and monodentate ligand (modulator). Such phenomenon has already been observed, and those defects may even lead to the higher permanent porosity and enhanced surface area.[90]

Conclusions and Outlook

Nowadays, Metal-Organic Frameworks are among the most studied porous materials. The increasing interest in these materials has been caused by their unique properties such as high surface area, tunable porosity, structural and topological diversity, and others, which allow the utilization of MOFs in a wide range of applications. However, traditional bulk materials are not always appropriate for some uses. Thus, efforts have been made to reduce the size of MOF particles to the nanoscale range. MOF nanocrystals not only may enhance the already known properties of bulk MOFs but also promote new features as a consequence of high surface-to-volume ratio and quantum size effects. Nevertheless, to establish factors leading to the controllable synthesis of MOF nanocrystals is a great challenge.

This review provides an overview of the different routes to synthesize MOF nanocrystals and to control their size and shapes. Many synthetic approaches such as direct precipitation, a solvo/hydrothermal method, an electrochemical method, and non-conventional approaches like a microwave or ultrasound-assisted synthesis were presented, and some of them were more indicated to prepare nanocrystals than the others. Among the reviewed synthetic methods, microwave and ultrasound-assisted methods are one of the most promising approaches to obtain uniform and well-dispersed MOF nanocrystals with narrow size distribution. Also, the use of additives, mainly coordinating modulators and surfactants plays a critical role in tuning the morphology of MOF nanocrystals. The control over the morphology of MOF particles is of utmost importance especially in medical applications such as drug delivery and imaging, and we believe that the synthesis of MOF nanocrystals will be a growing field in the MOF research in the near future.

Acknowledgments

The authors thank Federal University of Pernambuco and Brazilian agencies CNPq and FACEPE (Grant no. 407445/2013-7, 403747/2016-3, APQ-0818-1.06/15, PRONEX / FACEPE / CNPq Grant no. APQ-0675-1.06/14).

Conflict of Interest

The authors declare no conflict of interest.

Keywords: Control · Metal-Organic Frameworks · Morphology · Nanocrystals · Synthesis design

[1] J. U. A. H. Junghanns, R. H. Müller, *Int. J. Nanomedicine* **2008**, *3*, 295–309.
[2] P. Alivisatos, *Nat. Biotechnol.* **2004**, *22*, 47–52.
[3] V. Švrček, A. Slaoui, J. C. Muller, *Thin Solid Films* **2004**, *451–452*, 384–388.
[4] C. L. Torres-Martínez, R. Kho, O. I. Mian, R. K. Mehra, *J. Colloid Interface Sci.* **2001**, *240*, 525–532.
[5] R. S. de Oliveira, B. S. de Brito, J. Kulesza, S. Alves-Jr, B. S. Barros, *Ceram. Int.* **2017**, *43*, 8276–8283.
[6] Zeeya Merali, "This 1,600-Year-Old Goblet Shows that the Romans Were Nanotechnology Pioneers | History | Smithsonian," can be found under https://www.smithsonianmag.com/history/this-1600-year-old-goblet-shows-that-the-romans-were-nanotechnology-pioneers-787224/, **2013**.
[7] M. Faraday, *Philos. Trans. R. Soc. London* **1857**, *147*, 145–181.
[8] D. Thompson, *Gold Bull.* **2007**, *40*, 267–269.
[9] J. F. S. do Nascimento, B. S. Barros, J. Kulesza, J. B. L. de Oliveira, A. K. Pereira Leite, R. S. de Oliveira, *Mater. Chem. Phys.* **2017**, *190*, 166–174.
[10] A. Karina, P. Leite, B. Silva, J. Kulesza, J. Fagner, *Mater. Res.* **2017**, *20*, 681–687.
[11] "The Cambridge Structural Database Data Update - May 2017 - The Cambridge Crystallographic Data Centre (CCDC)," can be found under

https://www.ccdc.cam.ac.uk/support-and-resources/ccdcresources/csd-2017-updates/, **2017**.
[12] A. C. McKinlay, J. F. Eubank, S. Wuttke, B. Xiao, P. S. Wheatley, P. Bazin, J. C. Lavalley, M. Daturi, A. Vimont, G. De Weireld, et al., *Chem. Mater.* **2013**, *25*, 1592–1599.
[13] B. F. Hoskins, R. Robson, *J. Am. Chem. Soc.* **1990**, *112*, 1546–1554.
[14] R. Robson, B. F. Abrahams, S. R. Batten, R. W. Gable, B. F. Hoskins, J. Liu, in *Supramol. Archit.*, **1992**, pp. 256–273.
[15] P. Hubberstey, X. Lin, N. R. Champness, M. Schröder, in *Metal-Organic Frameworks: Design and Application,* John Wiley & Sons, Inc., Hoboken, New Jersey, **2010**, pp. 131–163.
[16] P. Dechambenoit, J. R. Long, *Chem. Soc. Rev.* **2011**, *40*, 3249–3265.
[17] X.-J. Wang, P.-Z. Li, Y. Chen, Q. Zhang, H. Zhang, X. X. Chan, R. Ganguly, Y. Li, J. Jiang, Y. Zhao, *Sci. Rep.* **2013**, *3*, 1149–1153.
[18] H. Ren, L. Zhang, J. An, T. Wang, L. Li, X. Si, L. He, X. Wu, C. Wang, Z. Su, *Chem. Commun.* **2014**, *50*, 1000–1002.
[19] Y.-B. Huang, J. Liang, X.-S. Wang, R. Cao, *Chem. Soc. Rev.* **2017**, *46*, 126–157.
[20] F.-Y. Yi, D. Chen, M.-K. Wu, L. Han, H.-L. Jiang, *ChemPlusChem* **2016**, *81*, 675–690.
[21] B. S. Barros, J. Chojnacki, A. A. Macêdo Soares, J. Kulesza, L. Lourenço Da Luz, S. A. Júnior, *Mater. Chem. Phys.* **2015**, *162*, 364–371.
[22] S. Muro, C. Garnacho, J. A. Champion, J. Leferovich, C. Gajewski, E. H. Schuchman, S. Mitragotri, V. R. Muzykantov, *Mol. Ther.* **2008**, *16*, 1450–1458.
[23] S. E. A. Gratton, P. A. Ropp, P. D. Pohlhaus, J. C. Luft, V. J. Madden, M. E. Napier, J. M. DeSimone, *Proc. Natl. Acad. Sci.* **2008**, *105*, 11613–11618.
[24] M. Giménez-Marqués, T. Hidalgo, C. Serre, P. Horcajada, *Coord. Chem. Rev.* **2015**, 342–360.
[25] C. P. Poole, F. J. Owens, *Introduction To Nanotechnology,* John Wiley & Sons, Inc., New Jersey, **2003**.
[26] Y. Xia, Y. Xiong, B. Lim, S. E. Skrabalak, *Angew. Chemie - Int. Ed.* **2009**, *48*, 60–103; *Angew. Chem.* **2009**,*121*, 60–108.
[27] S. Stevens, L. A. Sutherland, J. S. Krajcik, The Big Ideas of Nanoscale Science & Engineering: A Guidebook for Secondary Teachers, NSTA Press, Arlington, **2009**.
[28] G. Cao, Y. Wang, *Nanostructures and Nanomaterials - Synthesis, Properties and Applications*, World Scientific Publishing Co. Pte. Ltd, London, **2004**.
[29] R. Abazari, A. Reza Mahjoub, A. M. Z. Slawin, C. L. Carpenter-Warren, *Ultrason. Sonochem.* **2018**, *42*, 594–608.
[30] R. Abazari, A. R. Mahjoub, *Ultrason. Sonochem.* **2018**, *42*, 577–584.
[31] W. J. Rieter, K. M. L. Taylor, H. An, W. Lin, W. Lin, *J. Am. Chem. Soc.* **2006**, *128*, 9024–9025.
[32] K. M. L. Taylor, W. J. Rieter, W. Lin, *J. Am. Chem. Soc.* **2008**, *130*, 14358–14359.
[33] A. Cadiau, C. D. S. Brites, P. M. F. J. Costa, R. A. S. Ferreira, J. Rocha, L. D. Carlos, *ACS Nano* **2013**, *7*, 7213–7218.
[34] R. Xu, Y. Wang, X. Duan, K. Lu, D. Micheroni, A. Hu, W. Lin, *J. Am. Chem. Soc.* **2016**, *138*, 2158–2161.
[35] Y. Kataoka, K. Sato, Y. Miyazaki, K. Masuda, H. Tanaka, S. Naito, W. Mori, *Energy Environ. Sci.* **2009**, *2*, 397.
[36] N. T. K. Thanh, N. Maclean, S. Mahiddine, *Chem. Rev.* **2014**, *114*, 7610–7630.
[37] V. K. Lamer, R. H. Dinegar, *J. Am. Chem. Soc.* **1950**, *72*, 4847–4854.
[38] W. Ostwald, *Zeitschrift Fur Phys. Chemie–Stochiometrie Und Verwandtschaftslehre* **1900**, *34*, 495–503.
[39] J. Huo, M. Brightwell, S. El Hankari, A. Garai, D. Bradshaw, *J. Mater. Chem. A* **2013**, *1*, 15220–15223.
[40] C. W. Tsai, E. H. G. Langner, *Microporous Mesoporous Mater.* **2016**, *221*, 8–13.
[41] S. Dang, S. Song, J. Feng, H. Zhang, *Sci. China Chem.* **2015**, *58*, 973–978.
[42] L. A. Lozano, C. M. Iglesias, B. M. C. Faroldi, M. A. Ulla, J. M. Zamaro, *J. Mater. Sci.* **2017**, 1–12.
[43] B. Seoane, S. Castellanos, A. Dikhtiarenko, F. Kapteijn, J. Gascon, *Coordin. Chem. Rev.* **2016**, *307*, 147–187.
[44] M. Beetz, A. Zimpel, S. Wuttke, in *The Chemistry of Metal-Organic Frameworks, Synthesis, Characterization, and Applications,* Wiley-VCH Verlag GmbH & Co. KGaA, Weinheim, Germany, **2016**, pp. 491–521.
[45] Y. Pan, Y. Liu, G. Zeng, L. Zhao, Z. Lai, *Chem. Commun.* **2011**, *47*, 2071–2073.
[46] L. Na, L. Zhang, W. Zhang, R. Hua, *Synth. React. Inorganic, Met. Nano-Metal Chem.* **2015**, *45*, 1463–1466.
[47] J. Kulesza, B. S. Barros, I. M. V. da Silva, G. G. da Silva, S. Alves Júnior, *CrystEngComm* **2013**, *15*, 8881–8882.
[48] L. H. Wee, M. R. Lohe, N. Janssens, S. Kaskel, J. A. Martens, *J. Mater. Chem.* **2012**, *22*, 13742–13746.
[49] X. Li, Y. Liu, S. Liu, S. Wang, L. Xu, Z. Zhang, F. Luo, Y. Lu, S. Liu, *J. Mater. Chem. A* **2018**, *6*, 4678–4685.
[50] M. Oveisi, M. A. Asli, N. M. Mahmoodi, *J. Hazard. Mater.* **2018**, *347*, 123–140.
[51] E. Biemmi, S. Christian, N. Stock, T. Bein, *Microporous Mesoporous Mater.* **2009**, *117*, 111–117.
[52] J. W. P. Lindstrom, J. Tierney, B. Wathey, **2005**, *57*, 9225–9283.
[53] R. Vakili, S. Xu, N. Al-Janabi, P. Gorgojo, S. M. Holmes, X. Fan, *Microporous Mesoporous Mater.* **2018**, *260*, 45–53.
[54] A. Huang, L. Wan, J. Caro, *Mater. Res. Bull.* **2018**, *98*, 308–313.
[55] S. H. Jhung, J. Lee, J.-S. Chang, *Bull. Korean Chem. Soc.* **2005**, *26*, 880–881.
[56] J. Z. B. Liu, Y. He, L. Han, V. Singh, X. Xu, T. Guo, F. Meng. X. Xu, P. York, Z. Liu, *Cryst. Growth Des.* **2017**, *17*, 1654–1660.
[57] Y. Dong, H. Zhang, F. Lei, M. Liang, X. Qian, P. Shen, H. Xu, Z. Chen, J. Gao, J. Yao, *J. Solid State Chem.* **2017**, *245*, 160–163.
[58] J. Luo, X. Yang, S. Wang, Y. Bi, A. Nautiyal, X. Zhang, *Funct. Mater. Lett.* **2018**, *11*, 1850030–1-1850030–4.
[59] A. Laybourn, J. Katrib, R. S. Ferrari-John, C. G. Morris, S. Yang, O. Udoudo, T. L. Easun, C. Dodds, N. R. Champness, S. W. Kingman, et al., *J. Mater. Chem. A* **2017**, *5*, 7333–7338.
[60] O. Shekhah, J. Liu, R. A. Fischer, C. Wöll, *Chem. Soc. Rev.* **2011**, *40*, 1081–1106.
[61] A. F. F. Monteiro, Síntese de Cu–MOF's Via Método Eletroquímico: Caracterização E Aplicação Na Adsorção de Azul de Metileno, Federal University of Rio Grande do Norte, Natal, **2016**.
[62] H. Al-Kutubi, J. Gascon, E. J. R. Sudhölter, L. Rassaei, *ChemElectroChem* **2015**, *2*, 462–474.
[63] H. Yang, H. Du, L. Zhang, Z. Liang, W. Li, *Int. J. Electrochem. Sci.* **2015**, *10*, 1420–1433.
[64] S. D. Worrall, H. Mann, A. Rogers, M. A. Bissett, M. P. Attfield, R. A. W. Dryfe, *Electrochim. Acta* **2015**, *197*, 228–240.
[65] S. Khazalpour, V. Safarifard, A. Morsali, D. Nematollahi, *RSC Adv.* **2015**, *5*, 36547–36551.
[66] F. Zhang, T. Zhang, X. Zou, X. Liang, G. Zhu, F. Qu, *Solid State Ionics* **2017**, *301*, 125–132.
[67] L.-G. Qiu, Z.-Q. Li, Y. Wu, W. Wang, T. Xu, X. Jiang, *Chem. Commun.* **2008**, 3642–3644.
[68] V. Safarifard, A. Morsali, *Coordin. Chem. Rev.* **2015**, *292*, 1–14.
[69] M. Y. Masoomi, M. Bagheri, A. Morsali, *Ultrason. Sonochem.* **2016**, *33*, 54–60.
[70] N. Abdollahi, M. Y. Masoomi, A. Morsali, P. C. Junk, J. Wang, *Ultrason. Sonochem.* **2018**, *45*, 50–56.
[71] J. Kim, S.-T. Yang, S. B. Choi, J. Sim, J. Kim, W.-S. Ahn, *J. Mater. Chem.* **2011**, *21*, 3070–3076.
[72] G. G. da Silva, C. S. Silva, R. T. Ribeiro, C. M. Ronconi, B. S. Barros, J. L. Neves, S. A. Júnior, *Synth. Met.* **2016**, *220*, 369–373.
[73] M. Mohamedali, H. Ibrahim, A. Henni, *Chem. Eng. J.* **2018**, *334*, 817–828.
[74] I. Cota, F. Fernandez Martinez, *Coordin. Chem. Rev.* **2017**, *351*, 189–204.
[75] J. Liu, X. Zou, C. Liu, K. Cai, N. Zhao, W. Zheng, G. Zhu, *CrystEngComm* **2016**, *18*, 525–528.
[76] X. Sang, J. Zhang, J. Xiang, J. Cui, L. Zheng, J. Zhang, Z. Wu, Z. Li, G. Mo, Y. Xu, et al., *Nat. Commun.* **2017**, *8*, 1–7.
[77] D. Bradshaw, S. El-Hankari, L. Lupica-Spagnolo, *Chem. Soc. Rev.* **2014**, *43*, 5431–5443.
[78] K. M. Park, H. Kim, J. Murray, J. Koo, K. Kim, *Supramol. Chem.* **2017**, *29*, 441–445.
[79] G. Zheng, Z. Chen, K. Sentosun, I. Pérez-Juste, S. Bals, L. M. Liz-Marzán, I. Pastoriza-Santos, J. Pérez-Juste, M. Hong, *Nanoscale* **2017**, *9*, 16645–16651.
[80] X. Gao, R. Cui, M. Zhang, Z. Liu, *Mater. Lett.* **2017**, *197*, 217–220.
[81] S. P. Moulik, G. C. De, A. K. Panda, B. B. Bhowmik, A. R. Das, *Langmuir* **1999**, *15*, 8361–8367.
[82] W. Zheng, X. Hao, L. Zhao, W. Sun, *Ind. Eng. Chem. Res.* **2017**, *56*, 5899–5905.

[83] G. Sargazi, D. Afzali, A. Mostafavi, *Ultrason. Sonochem.* **2018**, *41*, 234–251.
[84] M. J. Katz, Z. J. Brown, Y. J. Colón, P. W. Siu, K. A. Scheidt, R. Q. Snurr, J. T. Hupp, O. K. Farha, *Chem. Commun.* **2013**, *49*, 9449–9451.
[85] A. Schaate, P. Roy, A. Godt, J. Lippke, F. Waltz, M. Wiebcke, P. Behrens, *Chem. - A Eur. J.* **2011**, *17*, 6643–6651.
[86] S. Diring, S. Furukawa, Y. Takashima, T. Tsuruoka, S. Kitagawa, *Chem. Mater.* **2010**, *22*, 4531–4538.
[87] J. Cravillon, R. Nayuk, S. Springer, A. Feldhoff, K. Huber, M. Wiebcke, *Chem. Mater.* **2011**, *23*, 2130–2141.
[88] S. Khazalpour, V. Safarifard, A. Morsali, D. Nematollahi, *Rsc Adv.* **2015**, *5*, 36547–36551.
[89] Y. P. Wu, W. Zhou, J. Zhao, W. W. Dong, Y. Q. Lan, D. S. Li, C. Sun, X. Bu, *Angew. Chemie - Int. Ed.* **2017**, *56*, 13001–13005; *Angew. Chem.* **2017**, *129*, 13181–13185.
[90] H. Wu, Y. S. Chua, V. Krungleviciute, M. Tyagi, P. Chen, T. Yildirim, W. Zhou, *J. Am. Chem. Soc.* **2013**, *135*, 10525–10532.

Submitted: May 11, 2018
Accepted: June 25, 2018